



**HAL**  
open science

## Woody debris is related to reach-scale hotspots of lowland stream ecosystem respiration under baseflow conditions

Pj. Blaen, M.J. Kurz, J.D. Drummond, J.L.A. Knapp, C. Mendoza Lera, N.M. Schmadel, M.J. Klaar, S. Folegot, J. Lee Cullin, A.S. Ward, et al.

### ► To cite this version:

Pj. Blaen, M.J. Kurz, J.D. Drummond, J.L.A. Knapp, C. Mendoza Lera, et al.. Woody debris is related to reach-scale hotspots of lowland stream ecosystem respiration under baseflow conditions. *Ecohydrology*, 2018, 11 (5), pp.e1952-. 10.1002/eco.1952 . hal-02608518

**HAL Id: hal-02608518**

**<https://hal.inrae.fr/hal-02608518v1>**




Submitted on 16 May 2020

**HAL** is a multi-disciplinary open access archive for the deposit and dissemination of scientific research documents, whether they are published or not. The documents may come from teaching and research institutions in France or abroad, or from public or private research centers.

L'archive ouverte pluridisciplinaire **HAL**, est destinée au dépôt et à la diffusion de documents scientifiques de niveau recherche, publiés ou non, émanant des établissements d'enseignement et de recherche français ou étrangers, des laboratoires publics ou privés.

## RESEARCH ARTICLE

# Woody debris is related to reach-scale hotspots of lowland stream ecosystem respiration under baseflow conditions

P.J. Blaen<sup>1,2</sup>  | M.J. Kurz<sup>3,11</sup> | J.D. Drummond<sup>4</sup> | J.L.A. Knapp<sup>5</sup> | C. Mendoza-Lera<sup>6,12</sup> | N.M. Schmadel<sup>7</sup> | M.J. Klaar<sup>8</sup> | A. Jäger<sup>9,13</sup> | S. Folegot<sup>1</sup> | J. Lee-Cullin<sup>10</sup> | A.S. Ward<sup>7</sup> | J.P. Zarnetske<sup>10</sup> | T. Datry<sup>6</sup> | A.M. Milner<sup>1</sup> | J. Lewandowski<sup>9,13</sup> | D.M. Hannah<sup>1</sup>  | S. Krause<sup>1,2</sup> 

<sup>1</sup>School of Geography, Earth and Environmental Sciences, University of Birmingham, Edgbaston, Birmingham B15 2TT, UK

<sup>2</sup>Birmingham Institute of Forest Research (BIFoR), University of Birmingham, Edgbaston, Birmingham B15 2TT, UK

<sup>3</sup>The Academy of Natural Sciences of Drexel University, Philadelphia, PA, USA

<sup>4</sup>Integrative Freshwater Ecology Group, Centre for Advanced Studies of Blanes (CEAB-CSIC), C/Accés a la Cala St Francesc, 17, Girona, Blanes 17300, Spain

<sup>5</sup>Universität Tübingen, Hölderlinstr. 12, Tübingen 72074, Germany

<sup>6</sup>Irstea, UR RiverLy, centre de Lyon-Villeurbanne, Villeurbanne 69625, France

<sup>7</sup>School of Public and Environmental Affairs, Indiana University, 430 MSB-II, Bloomington, IN 47405, USA

<sup>8</sup>School of Geography, University of Leeds, Leeds LS2 9JT, UK

<sup>9</sup>Leibniz-Institute of Freshwater Ecology and Inland Fisheries, Müggelseedamm 310, Berlin 12587, Germany

<sup>10</sup>Department of Earth and Environmental Sciences, Michigan State University, East Lansing, MI 48824, USA

<sup>11</sup>Helmholtz Centre for Environmental Research (UFZ), Leipzig, Germany

<sup>12</sup>Department of Freshwater Conservation, Brandenburg University of Technology Cottbus-Senftenberg, Seestraße 45, Bad Saarow 10435, Germany

<sup>13</sup>Geography Department, Humboldt University Berlin, Berlin 10099, Germany

## Correspondence

Phillip Blaen, School of Geography, Earth and Environmental Sciences, University of Birmingham, Edgbaston, Birmingham B15 2TT, UK.

Email: p.j.blaen@bham.ac.uk

## Funding information

Natural Environment Research Council, Grant/Award Number: NE/L003872/1; Birmingham Institute for Forest Research; UK Natural Environment Research Council, Grant/Award Number: NERC NE/L003872/1; Leverhulme Trust, Grant/Award Number: Where rivers, groundwater and disciplines meet: a

## Abstract

Stream metabolism is a fundamental, integrative indicator of aquatic ecosystem functioning. However, it is not well understood how heterogeneity in physical channel form, particularly in relation to and caused by in-stream woody debris, regulates stream metabolism in lowland streams. We combined conservative and reactive stream tracers to investigate relationships between patterns in stream channel morphology and hydrological transport (*form*) and metabolic processes as characterized by ecosystem respiration (*function*) in a forested lowland stream at baseflow. Stream reach-scale ecosystem respiration was related to locations (“hotspots”) with a high abundance of woody debris. In contrast, nearly all other measured hydrological and geomorphic variables previously documented or hypothesized to influence stream metabolism did not significantly explain ecosystem respiration. Our results suggest the existence of key differences in physical controls on ecosystem respiration between lowland stream systems (this study) and smaller upland streams (most previous studies) under baseflow conditions. As such, these findings have implications for reactive transport models that predict biogeochemical transformation rates from hydraulic transport parameters, for upscaling frameworks that represent biological stream processes at larger network scales, and for the effective management and restoration of aquatic ecosystems.

## KEYWORDS

ecosystem respiration, hydrological tracer, solute transport, stream metabolism, woody debris

This is an open access article under the terms of the Creative Commons Attribution License, which permits use, distribution and reproduction in any medium, provided the original work is properly cited.

© 2018 The Authors. *Ecohydrology* published by John Wiley & Sons Ltd.

## 1 | INTRODUCTION

In-stream processing by aquatic communities constitutes an important control on the export of nutrients and organic matter from landscapes (Mulholland et al., 2008) and the atmospheric evasion of greenhouse gases from water bodies (Cole et al., 2007). In watersheds enriched by nutrients, in-stream processing can mitigate eutrophication of downstream ecosystems. Contemporary research indicates small steep headwater streams are highly effective in removing nutrients from fluvial networks (Mulholland et al., 2008). In contrast, low-gradient lowland stream systems are understudied relative to headwaters (Dodds et al., 2013). These lowland streams require more study because they are often characterized by high nutrient loads due to intensive agricultural activities in lowland areas, and, thus, these streams are potentially of more relevance to river managers than less-impacted headwaters (Rode, Halbedel NéE Angelstein, Anis, Borchardt, & Weitere, 2016; Tank, Rosi-Marshall, Baker, & Hall, 2008).

The processing of nutrients and organic matter in stream ecosystems is closely linked to metabolic processes (e.g., Tank, Rosi-Marshall, Griffiths, Entekin, & Stephen, 2010). As such, ecosystem metabolism (i.e., the balance of primary production and ecosystem respiration) represents a valuable functional indicator to better understand controls on aquatic nutrient processing. In particular, estimates of ecosystem respiration are very informative in heterotrophic systems where respiration dominates the oxygen budget. However, obtaining accurate respiration rates remains one of the biggest challenges for measuring and predicting biogeochemical cycling in aquatic ecosystems (Hotchkiss & Hall Jr, 2014).

Research to date, conducted mainly in small, upland headwater streams, indicates that ecosystem respiration may be influenced by physical channel forms across a range of scales: from individual geomorphic units (Cardinale, Palmer, Swan, Brooks, & Poff, 2002) through stream reaches to whole basins (Mulholland et al., 2001). For example, Cardinale et al. (2002) recorded increased benthic biofilm respiration in riffles with greater physical heterogeneity, whereas Fellows, Valett, and Dahm (2001) demonstrated that increased hyporheic exchange and transient storage were associated with an increase in ecosystem respiration in two headwater streams. In particular, in-stream woody debris has strong potential to influence ecosystem respiration through several different processes. Dixon and Sear (2014) and Krause et al. (2014) highlighted how woody debris emplaced during baseflow conditions may trap sediments and alter hydrodynamic and hydrostatic forcing, thus increasing hyporheic exchange fluxes supplying nutrients and oxygen to hyporheic microbial communities that contribute to stream ecosystem respiration. Alternatively, woody debris features may stimulate ecosystem respiration by increasing channel transient storage (Jin, Siegel, Lautz, & Otz, 2009) or by acting as a substrate for biofilms (Battin et al., 2008).

Currently, there is limited understanding as to how heterogeneity in physical channel form, particularly in relation to in-stream woody debris, regulates stream respiratory function in lowland streams. Woody debris conditions of large lowland stream reaches can contrast markedly with upland reaches (Gomi, Sidle, & Richardson, 2002). In lowland streams, which are less constrained by their valleys, woody debris may not drive pressure head differences and influence

hyporheic exchange to the same extent as in small, steep headwaters because channel-spanning debris dams are comparatively rare in large, lowland streams (Dixon & Sear, 2014). Nonetheless, woody debris may still be an important control on ecosystem respiration in lowland streams, particularly at low flows when overall valley-bottom hydraulic residence times are typically higher (Boano et al., 2014). For example, woody debris can retain sediments and thus alter in-stream solute transport pathways. Moreover, increased levels of nutrients and organic matter in lowland streams relative to headwaters often correspond to the increased influence of physical conditions in driving ecosystem respiration, as opposed to biogeochemical conditions, than in headwater streams where nutrient and organic matter availability are more limiting (Krause et al., 2014).

To address these research gaps, we investigated the relationships between spatial patterns in hydrological stream solute transport and channel geomorphology (*form*) and stream ecosystem respiration dynamics (*function*) in a relatively slow-flowing lowland stream containing abundant woody debris features. We hypothesized: (a) that solute patterns of reaches within this stream, such as transient storage, advection, and dispersion, would be related to in-stream woody debris and the overall reach channel morphology; and (b) that the presence and abundance of in-stream woody debris would increase rates of reach-scale ecosystem respiration. To test these hypotheses, we combined conservative and reactive fluorescent tracers to assess spatial variability in both physical transport processes and ecosystem respiration across subreaches with varying morphology and wood-debris conditions nested within a 1-km lowland stream reach.

## 2 | METHODS

### 2.1 | Site description

Our experiment was conducted in late spring during June 2015 in the Hammer Stream in West Sussex, United Kingdom. The 24.6 km<sup>2</sup> stream catchment is composed of mixed-use agricultural land interspersed with deciduous broad-leaved woodland, and sandstone and mudstone geology. The stream was at baseflow (discharge  $\approx 70 \text{ L s}^{-1}$ ) for 7 days preceding, as well as throughout, the study period. A 1-km study reach was established within a deciduous forested valley (Figure 1). The reach was characterized by sand-dominated bed sediments and a meandering morphology, which produced heterogeneous areas of shallow, fast-flowing water interspersed with deeper pools with lower flow velocities under baseflow conditions. In some sections, woody debris trapped and retained river sediments, which generated head differences that altered flow dynamics around these bedform features. The gradient of the reach was relatively low throughout its length ( $-0.24$  to  $-1.05 \text{ mm/m}$ ; Table 1); field observations indicated that even the steepest subreach surface water gradients were not sufficient to induce visible supercritical flows that caused mechanical reaeration (i.e., no observed highly turbulent or standing wave locations), except for around some of the woody debris features. See Text S1 for further site and flow condition details.

## 2.2 | Subreach geomorphology and sediment characterization

Five subreaches were established with contrasting geomorphology and sediment characteristics (Figure 1). Longitudinal distances and channel widths were surveyed for each subreach, and mean values were combined with discharge measured by tracer experiments (described below) to inversely calculate mean depths for each subreach. Slope, sinuosity, bed sediment particle size distributions, and the abundance and characteristics of in-stream woody debris (>20 mm diameter and >0.6 m length) were also surveyed for each subreach. See Text S2 for full measurement details.

## 2.3 | Solute tracer experiments

A dual stream solute tracer slug injection was conducted using 10 g Uranine as a conservative tracer and 40 g Resazurin (Raz) as a reactive

tracer, targeting a peak upstream concentration of 50 and 100 ppb, respectively. Raz is a weakly fluorescent metabolically active compound that transforms irreversibly to highly fluorescent Resorufin (Rru) under mildly reducing conditions, most commonly in the presence of aerobic microorganisms (Haggerty, Argerich, & Martí, 2008). Accordingly, the rate of Raz–Rru transformation represents an integrated measure of (near-instantaneous) whole-stream ecosystem respiration (González-Pinzón, Haggerty, & Argerich, 2014).

Tracers were co-injected instantaneously, and concentration breakthrough curves (BTCs) of Uranine, Raz, and Rru were measured at six locations along the study reach (Figure 1). In contrast to many previous field studies that have quantified Raz and Rru from discrete grab samples and laboratory analysis, for example (González-Pinzón et al., 2014), this study measured tracer BTCs using in situ field fluorimeters (GGUN-FL30, Albillia Sàrl, Switzerland) positioned in the thalweg of each subreach at 10 s resolution (Lemke, Schnegg, Schwientek, Osenbrück, & Cirpka, 2013), thereby enabling insights

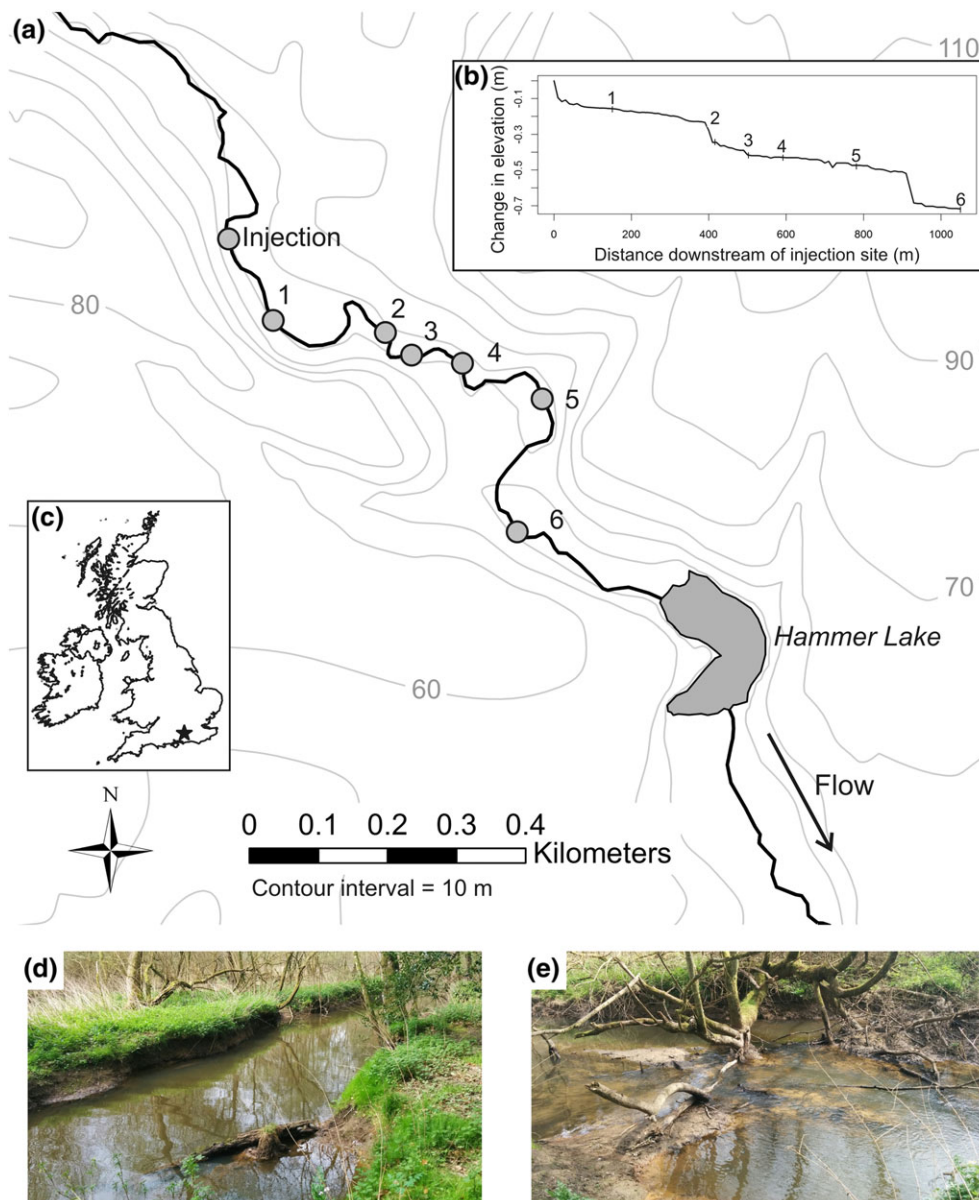


**FIGURE 1** Overview of study site showing (a) study reach and monitoring locations; (b) slope profile; (c) location of site in UK; (d) image of stream; and (e) example of in-stream woody debris. The five subreaches correspond to stream sections between monitoring locations (i.e., 1–2 and 2–3)

**TABLE 1** Physical and geomorphic characteristics for subreaches within the study reach

| Subreach    | Length<br>m | Mean<br>water<br>depth<br>m | Mean<br>channel<br>width<br>m | Mean gradient<br>mm/m | Median<br>flow<br>velocity<br>m/s | Sinuosity<br>m/m | Sediment grain size % |          |             |               | Subreach description |                                                                                                       |
|-------------|-------------|-----------------------------|-------------------------------|-----------------------|-----------------------------------|------------------|-----------------------|----------|-------------|---------------|----------------------|-------------------------------------------------------------------------------------------------------|
|             |             |                             |                               |                       |                                   |                  | >2 mm                 | 0.5–2 mm | 0.25–0.5 mm | 0.063–0.25 mm |                      | <0.063 mm                                                                                             |
| Injection–1 | 150         | 0.58                        | 5.31                          | –1.05                 | 0.02                              | 1.13             | 2                     | 33       | 18          | 41            | 6                    | Deep, wide, slow-flowing with little in-channel flow variability                                      |
| 1–2         | 260         | 0.17                        | 4.93                          | –0.73                 | 0.09                              | 1.60             | 0                     | 2        | 80          | 17            | 1                    | Shallow, relatively fast water flow, occasional debris dams                                           |
| 2–3         | 90          | 0.19                        | 4.95                          | –0.78                 | 0.08                              | 1.84             | 1                     | 0        | 88          | 8             | 2                    | Frequent in-channel obstructions, evidence of sediment accumulation and scouring                      |
| 3–4         | 90          | 0.48                        | 6.02                          | –0.14                 | 0.02                              | 1.22             | 1                     | 31       | 66          | 2             | 1                    | Wide, slow-flowing, several fully submerged debris pieces                                             |
| 4–5         | 190         | 0.77                        | 5.58                          | –0.24                 | 0.02                              | 1.35             | 0                     | 0        | 89          | 9             | 2                    | Deep, wide, slow-flowing with occasional large debris dams                                            |
| 5–6         | 270         | 0.24                        | 5.50                          | –0.90                 | 0.05                              | 1.37             | 2                     | 4        | 55          | 16            | 23                   | Frequent in-channel obstructions, evidence of sediment accumulation, high in-channel flow variability |

into tracer dynamics at a much higher resolution than possible using a manual sampling approach. See Text S3 for full measurement details.

## 2.4 | Conservative tracer hydrodynamic modelling and calculation of transient storage metrics

A hydrodynamic model, the stochastic mobile–immobile model, was fitted to each Uranine BTC to characterize solute transport and retention characteristics (Boano et al., 2014). The input boundary condition was the BTC immediately upstream of the modelled site (i.e., the Site 1 BTC was the input to Site 2). Thus, model analysis was performed for each subreach in a downstream sequential pattern (i.e., 1–2, 2–3, 3–4, and so on).

Parametric modelling approaches to quantify stream solute transport dynamics can be uncertain and susceptible to equifinality (Ward et al., 2013). Therefore, Uranine BTCs were also characterized by their temporal characteristics to provide further metrics (below) to compare spatial variability in solute transport dynamics within and between subreaches. Normalized by advective time, transient storage indices ( $TSI_{norm}$ ), coefficients of variation (CV), and skewness were estimated for each BTC following Ward et al. (2013). Differences in temporal metrics ( $\Delta TSI_{norm}$ ,  $\Delta CV$ ,  $\Delta Skewness$ ) between BTCs at the upstream and the downstream end of each subreach (i.e., between Sites 1 and 2, Sites 2 and 3, and so on) were then estimated following Schmadel et al. (2016) to examine the influence of individual subreaches on solute transport process variability. See Text S4 for further details.

## 2.5 | Reactive tracer modelling and analysis

The Raz tracer system was used to indicate relative differences in metabolic activity between subreaches within the study stream reach. Estimates of Raz and Rru mass recovery were adjusted for potential changes in discharge through the study reach by correcting for conservative tracer (i.e., Uranine) mass recovery. Thus, Raz–Rru transformation rate coefficients were estimated for each subreach as:

$$\lambda_{raz \rightarrow rru}^* = \frac{1}{\tau} \ln \left( \frac{\mu_{0,up}^{raz}}{\mu_{0,up}^{raz} + \mu_{0,up}^{rru} - \mu_{0,dn}^{rru}} \right), \quad (1)$$

where  $\lambda_{raz \rightarrow rru}^*$  (1/s) is the Raz–Rru transformation rate coefficient in the subreach,  $\mu_{0,up}^{raz}$  and  $\mu_{0,up}^{rru}$  (mg s/L) are the zeroth temporal moments (the integral of concentration with respect to time) for Raz and Rru, respectively, at the upstream end of each subreach,  $\mu_{0,dn}^{rru}$  is the zeroth order temporal moment for Rru at the downstream end of each subreach, and  $\tau$  (s) is the median travel time in the subreach as calculated from the first temporal moment of each BTC following Schmadel et al. (2016). Normalizing Raz–Rru transformation values by advective time produces rate estimates that are independent of subreach length and flow velocity.

In contrast to most previous studies that have focused solely on Raz decay (e.g., González-Pinzón et al., 2014), this approach utilizes information of both Raz and Rru BTCs because detection accuracies of the field fluorometers were higher for highly fluorescent Rru than for relatively low-fluorescent Raz (Knapp & Cirpka, 2017). Irreversible

sorption of the tracer was not accounted for because all tracers were expected to have similar sorption properties under the mildly alkaline conditions present (Haggerty et al., 2008).

## 2.6 | Data analysis

To investigate linkages between physical channel form variability, hydrological parameters, and ecosystem respiration, Raz–Rru transformation rate coefficients were regressed against conservative tracer model results, BTC metrics, and stream geomorphic characteristics conducted using the statistical software R version 3.1.1 (R Core Team, 2016). Relationships were considered significant if 95% confidence intervals (calculated from standard errors of slope estimates) of regression model parameters did not include zero. Additional nonparametric statistical tests for differences (Wilcoxon signed ranks test) and relationships (Spearman's rank-order correlation) between measured variables were performed due to the relatively small number of cases and the potential for nonnormal data distributions.

## 3 | RESULTS

### 3.1 | Stream hydrologic, geomorphic, and woody debris characteristics

Stream discharge during the experiment was estimated as  $73.2 \text{ L s}^{-1}$  from the Uranine BTC at Site 1. The proportion of conservative tracer mass recovered did not change considerably with travel distance; estimates from Uranine BTC zeroth temporal moments ranged from 0.95 to 1.11. Median flow velocities, determined by travel times from Uranine BTC first temporal moments, ranged from  $0.02 \text{ m s}^{-1}$  in Subreach 4–5 to  $0.09 \text{ m s}^{-1}$  in Subreach 1–2 (Table 1) and exhibited significant ( $p < .05$ ) negative relationships with stream depth ( $r = -0.88$ ) and width ( $r = -0.91$ ). Sediment grain size distributions were similar along the whole stream reach with sand particles (0.063–2 mm) accounting for most of the sediment fraction in all subreaches (Table 1). The abundance of woody debris ranged from 0.1 pieces  $\text{m}^{-1}$  in Subreach 3–4 to 0.23 pieces  $\text{m}^{-1}$  in Subreach 2–3 (Table 2; Figure 2). The majority of woody debris pieces were <100 mm diameter and partially buried (anchored) in bed sediments. Relatively few debris pieces spanned the entire channel cross section (<20% of total debris).

### 3.2 | Stream solute transport dynamics and hydrodynamic modelling

Raz mass recoveries exhibited no significant trend with travel time throughout the study reach. However, Rru peak concentrations and mass detection increased from upstream to downstream, indicating Raz–Rru transformation occurred along the flowpath (Figure 3a). Tracer BTCs exhibited similar tailing behaviour throughout the study reach with the exception of Site 4 where tracer mass was slightly delayed relative to other sites (Figure 3b,c). When normalized by their zeroth temporal moments, Uranine and Raz solute dynamics appeared virtually identical (Figure 3b). In contrast, Rru dynamics were delayed markedly for mean arrival times relative to Uranine (Wilcoxon signed-rank test  $Z = -2.21$ ,  $p < .05$ ) and Raz ( $Z = -2.20$ ,  $p < .05$ ).

Stochastic mobile–immobile model simulations represented the system well (Table 3; Figure 3c) with Nash–Sutcliffe efficiency coefficients  $>0.98$  for all model fits. However, BTC tailing at Site 4 was not as well characterized as for the other BTCs. Stream velocity was positively related to dispersion ( $r = 0.88$ ,  $p < .05$ ). Péclet numbers derived from tracer modelling results were high ( $>5$ ) for all BTCs, indicating advection dominated solute dynamics throughout the study

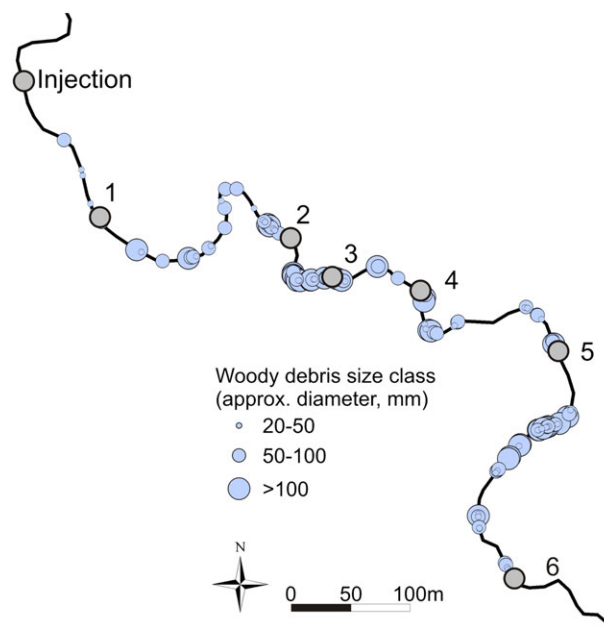


**FIGURE 2** Distribution of observed in-stream woody debris within the study reach. Numbers indicate tracer monitoring locations

**TABLE 2** Woody debris characteristics for subreaches within the study reach

| Subreach    | Total abundance<br>pieces/m | Diameter size fraction |                |              | Channel<br>spanning<br>% | Partially<br>buried<br>% | Fully<br>submerged<br>% | Longitudinal<br>distribution CV |
|-------------|-----------------------------|------------------------|----------------|--------------|--------------------------|--------------------------|-------------------------|---------------------------------|
|             |                             | 20–50 mm<br>%          | 50–100 mm<br>% | >100 mm<br>% |                          |                          |                         |                                 |
| Injection–1 | 0.04                        | 83.3                   | 16.7           | 0.0          | 0.0                      | 100.0                    | 0.0                     | 24.7                            |
| 1–2         | 0.12                        | 37.5                   | 46.9           | 15.6         | 21.9                     | 93.8                     | 9.4                     | 46.4                            |
| 2–3         | 0.23                        | 23.8                   | 33.3           | 42.9         | 19.1                     | 100.0                    | 19.0                    | 40.6                            |
| 3–4         | 0.10                        | 11.1                   | 55.6           | 33.3         | 22.2                     | 88.9                     | 22.2                    | 98.8                            |
| 4–5         | 0.14                        | 37.5                   | 41.7           | 20.8         | 29.2                     | 95.8                     | 16.7                    | 71.6                            |
| 5–6         | 0.17                        | 40.9                   | 31.8           | 27.3         | 18.2                     | 81.8                     | 4.5                     | 45.6                            |

Note. CV = coefficient of variation.

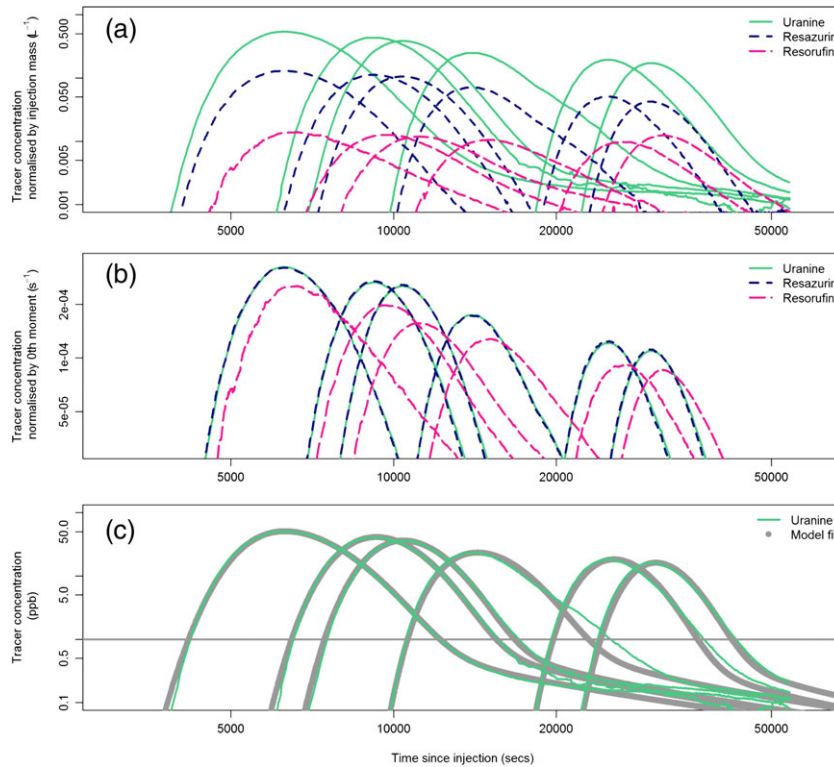


**FIGURE 3** (a) Tracer breakthrough curves (BTCs) for Uranine, Resazurin, and Resorufin at six monitoring locations normalized by molar injection mass; (b) tracer BTCs normalized by 0th moment; and (c) Uranine BTCs plotted with stochastic mobile-immobile model simulation results. The horizontal grey line indicates the 1 ppb truncation level applied to field data for the purpose of calculating BTC metrics

**TABLE 3** Best-fit parameters from SMIM simulation outputs and Raz-Rru transformation rates for each subreach

| Subreach | Length<br>m | Modelled velocity<br>m/s | Dispersion<br>m/s <sup>2</sup> | $\Lambda$<br>1/s | $\beta$ | Raz-Rru transformation rate<br>/day |
|----------|-------------|--------------------------|--------------------------------|------------------|---------|-------------------------------------|
| 1-2      | 260         | 0.089                    | 0.620                          | 1.80E-04         | 0.4     | 0.78                                |
| 2-3      | 90          | 0.078                    | 0.360                          | 7.00E-04         | 0.4     | 3.39                                |
| 3-4      | 90          | 0.024                    | 0.090                          | 4.00E-04         | 0.4     | 0.62                                |
| 4-5      | 190         | 0.017                    | 0.054                          | 1.00E-05         | 0.4     | 0.27                                |
| 5-6      | 270         | 0.052                    | 0.515                          | 1.50E-04         | 0.4     | 1.93                                |

Note.  $\Lambda$  = exchange rate of solute with the immobile zone;  $\beta$  = power-law exponent; SMIM = stochastic mobile-immobile model.

reach. Patterns in BTC metrics ( $\Delta TSI_{norm}$ ,  $\Delta CV$ ,  $\Delta Skewness$ ) were not correlated with most measured geomorphic or hydrological characteristics, with the exception of  $\Delta Skewness$  that was positively related to the rate of solute exchange into the immobile zone,  $\Lambda$  ( $r = 0.98$ ,  $p < .01$ ).

### 3.3 | Ecosystem respiration conditions

Raz-Rru transformation rate coefficients ( $\lambda_{raz \rightarrow rru}^*$ ), which are indicative of ecosystem respiration, for each subreach ranged between 0.27 and 3.39 day<sup>-1</sup> (Table 3). There was a marked separation between subreaches with relatively low transformation rates (1-2; 3-4; 4-5) and those with relatively higher rates (2-3; 5-6). Raz-Rru transformation rate coefficients did not exhibit significant relationships with the majority of measured geomorphic variables or metrics of transient storage (Table 4). However, transformation rate coefficients were significantly positively correlated with the abundance of woody debris present in each subreach ( $r = 0.84$ ,  $p < .05$ ; Figure 4; Table 4).

## 4 | DISCUSSION AND IMPLICATIONS

### 4.1 | Physical controls on stream solute transport

Conservative and reactive tracer BTCs captured at high temporal resolution facilitated detailed insights into solute transport and ecosystem respiration dynamics through the study reach. All conservative tracer BTCs followed a power-law slope tailing behaviour, indicating that the slowest solute release process was controlled by the same factor as predicted by stochastic theory (Schumer, Meerschaert, & Baeumer, 2009). Transport through hyporheic sediments has been shown to characterize late-time tailing behaviour of in-stream BTCs (Drummond et al., 2012). The power-law tailing behaviour observed within this study most likely represents the homogenous near-surface sandy substrate present throughout the entire 1-km stream reach. The delayed behaviour of Rru relative to both Uranine and Raz is presumed to reflect the time required for Raz to enter biologically active zones within the stream reach, to undergo transformation to Rru, and then to return to the main channel.

**TABLE 4** Correlations between Raz–Rru transformation rate coefficients and measured hydrological and geomorphic variables

| Category                       | Variable            | Observed relationship with Raz–Rru transformation rate coefficient | R <sup>2</sup> | p           |
|--------------------------------|---------------------|--------------------------------------------------------------------|----------------|-------------|
| Hydrological                   | Velocity            | +                                                                  | 0.272          | .368        |
|                                | $\Delta TSI_{norm}$ | =                                                                  | 0.055          | .704        |
|                                | $\Delta CV$         | +                                                                  | 0.118          | .572        |
|                                | $\Delta Skewness$   | +                                                                  | 0.542          | .156        |
|                                | Dispersion          | +                                                                  | 0.139          | .537        |
|                                | $\Lambda$           | +                                                                  | 0.571          | .140        |
|                                | Geomorphic          | Depth                                                              | –              | 0.396       |
| Width                          |                     | –                                                                  | 0.201          | .449        |
| Gradient                       |                     | –                                                                  | 0.498          | .183        |
| Sinuosity                      |                     | +                                                                  | 0.438          | .224        |
| <b>Woody debris: Abundance</b> |                     | <b>+</b>                                                           | <b>0.840</b>   | <b>.029</b> |
| Woody debris: Span             |                     | –                                                                  | 0.528          | .165        |
| Woody debris: Buried           |                     | =                                                                  | 0.044          | .734        |
| Woody debris: Fully submerged  |                     | =                                                                  | 0.002          | .941        |
| Woody debris: CV distribution  |                     | –                                                                  | 0.422          | .235        |

Note. Relationships were categorized as positive ( $r > 0.3$ ), negative ( $r < -0.3$ ), or equal ( $-0.3 < r < 0.3$ ). Bold text indicates a statistically significant correlation ( $p < .05$ ).

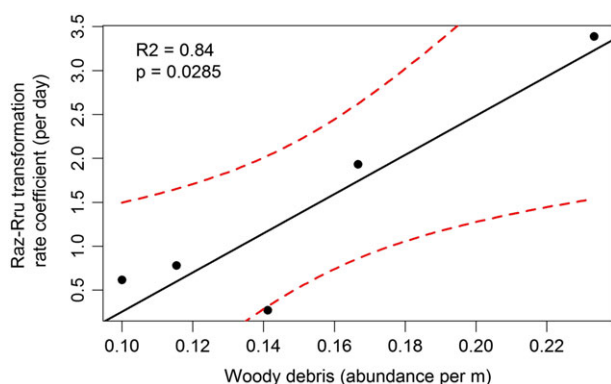


**FIGURE 4** Relationships between Raz–Rru transformation rate coefficients ( $\text{day}^{-1}$ ) and in-channel woody debris ( $\text{abundance m}^{-1}$ ). Dashed red lines indicate regression model 95% confidence intervals

In general, we found little evidence to support our first hypothesis (i.e., that patterns of solute transport would be strongly related to changes in channel form or woody debris), likely due to advection being the dominant process that obscures subtle transient storage differences created by channel morphology and wood as suggested by Schmadel et al. (2016). This outcome is unexpected because large wood features (e.g., log jams and beaver dams) can control stream solute transport dynamics significantly by altering head differences, increasing channel roughness and reducing downstream transport rates (Jin et al., 2009), and thereby promote transient storage within stream environments. In the present study, subreach differences in the abundance of in-channel woody debris did not appear to significantly influence short-term hydrologic storage processes operating along the flow path. This may have resulted from the relatively slow flow velocities and that woody debris did not effectively block channel cross sections in the study reach to the same degree as other studies (Jin et al., 2009), limiting the potential for woody debris to significantly influence solute storage dynamics under baseflow conditions. It is also worth noting that the spatial distribution and abundance of woody debris in the study reach was very similar to that observed in both smaller headwater forested streams (Curran & Wohl, 2003) and also to larger lowland streams (Piégay & Gurnell, 1997). Thus, spatial

distribution and abundance of woody debris may not be as significant a predictor of solute transport conditions, such as transient storage, as how woody debris is arranged in the channel and how it alters the local flow field (e.g., partial or fully channel spanning).

## 4.2 | Subreach patterns of ecosystem respiration

Raz–Rru transformation rate coefficients varied considerably for different subreaches. Three of the five subreaches exhibited relatively low transformation rates, potentially reflecting a “baseline” level of ecosystem respiration. In contrast, two other reaches were metabolic hotspots with transformation rates 3–4 times greater than observed elsewhere in the stream. These rates provide surrogate indicators of ecosystem respiration because experiments show Raz–Rru transformation is directly proportional to cellular respiration as represented by dissolved oxygen consumption (González-Pinzón et al., 2014). Although the molar processing ratio of oxygen to Raz is ecosystem-dependent, application of published values (González-Pinzón et al., 2014; González-Pinzón, Peipoch, Haggerty, Martí, & Fleckenstein, 2016) to the present study suggests respiration rates ranged from 0.17 to 0.30  $\text{day}^{-1}$  in the least reactive subreach (4–5) and between 2.10 and 3.77  $\text{day}^{-1}$  in the most reactive subreach (2–3). These transformation rates are very similar to those observed by other tracer studies in both lowland and upland streams (e.g., González-Pinzón et al., 2014; Knapp & Círpka, 2017) suggesting ecosystem respiration in lowland rivers may be comparable to headwaters (Tank et al., 2008).

## 4.3 | Hydro-geomorphic influences on ecosystem respiration

The positive correlation observed between Raz turnover and woody debris suggests that stream sections with a higher abundance of in-channel woody debris may have facilitated the development of hotspots of ecosystem respiration within our lowland forested stream reach under baseflow conditions, supporting our second hypothesis. The processes underpinning this relationship are not certain but do not appear to be caused by woody debris increasing localized transient storage due to the lack of significant relationships observed between



Raz–Rru transformation, woody debris, and hydrological transport metrics. Although there are several biotic and abiotic factors that could potentially account for this relationship, we suggest that the relatively stable spatial nature of flow along this lowland stream channel, coupled with very low biogeochemical variability in surface water between subreaches, indicates that the presence of woody debris may induce localized turbulence and increased advective mass transfer of nutrients and oxygen into the hyporheic zone, in turn increasing the contribution of hyporheic communities to ecosystem respiration (Krause et al., 2014; Mendoza-Lera et al., 2017). Alternatively, woody debris may act as a substrate and carbon source for epixylic biofilms that represent localized in-channel zones of ecosystem respiration (Battin et al., 2008).

Inconsistent with the observed relationship with woody debris, Raz–Rru transformation rates were not significantly related to most other measured geomorphic variables or metrics of transient storage. In contrast, previous studies conducted in headwater streams have demonstrated close links between physical properties and ecosystem respiration (e.g., Fellows et al., 2001). It may be that differences in geomorphology and solute transport between subreaches were not sufficiently different to have a discernible influence on ecosystem respiration. However, heterogeneity in many variables (e.g., sinuosity and gradient) was similar to, and in some cases higher than, previously reported values for lowland stream systems elsewhere in the UK (Piégay & Gurnell, 1997). As such, we consider our study reach to be broadly representative of forested lowland streams in this region and therefore suggest that the processes that influence ecosystem respiration in lowland streams may be different from those in smaller headwater ecosystems.

#### 4.4 | Implications and future directions

The quantification of relationships to understand how hydrological transport and physical channel form regulate stream ecosystem functioning is a major gap within the aquatic sciences, particularly for lowland stream environments that have been relatively neglected compared with upland headwaters. Our study contributes to addressing this knowledge deficit by examining interactions between physical morphology, hydrological transport, and stream metabolism. Although stream metabolism is often controlled in the first instance by the availability of organic matter, our results highlight the potential importance of woody debris in creating reach-scale hotspots of ecosystem respiration in this forested lowland study stream under baseflow conditions. Given the tight coupling between stream metabolism and biogeochemical cycling (Tank et al., 2010), this finding may have potential implications for river management and restoration activities aimed towards improving the chemical and ecological status of river ecosystems (Buss et al., 2009). For example, if these observed relationships hold across a range of lowland stream environments and flow conditions, then targeted additions of woody debris to river channels may have the potential to reduce nutrient loading of receiving surface waters and may also create wider environmental benefits in light of the positive contribution made by woody debris to other ecosystem processes such as erosion control and flood risk mitigation (Krause et al., 2014).

In a wider context, identifying controls on ecosystem respiration is relevant to developing frameworks to upscale rates of biogeochemical cycling and improve predictions of river nutrient attenuation capacity (e.g., through reactive transport models) at network scales (Grizzetti et al., 2015). Moreover, given the important role of river networks in connecting atmospheric, terrestrial, and marine systems (Cole et al., 2007), this research will contribute to our knowledge of global biogeochemical cycling, for example, by adding to our understanding of the potential for greenhouse gas emissions from terrestrial freshwater ecosystems (Battin et al., 2008).

Finally, our findings suggest avenues for future research agendas to identify the specific nature of the processes that underpin our observations of links between woody debris and stream ecosystem respiration. For example, given that woody debris can become mobile under high flow conditions (Dixon & Sear, 2014), understanding how temporal changes in woody debris distribution affect ecosystem respiration hotspot locations will be an important next step for further research in this field. In addition, further studies contrasting controls on metabolic processes between headwater and lowland streams environments are required to develop our conceptual understanding of ecosystem organization at whole-catchment scales. Addressing these knowledge gaps will generate a more thorough process-based understanding of the linkages between physical channel forms and ecosystem functioning within stream networks and improve our capacity to manage and restore aquatic ecosystems effectively.

#### ACKNOWLEDGEMENTS

Funding was provided by the Leverhulme Trust (*Where rivers, groundwater and disciplines meet: a hyporheic research network*), the UK Natural Environment Research Council (*Large woody debris—A river restoration panacea for streambed nitrate attenuation?* NERC NE/L003872/1), and the Birmingham Institute for Forest Research (BIFoR paper number 35). We also extend our thanks to the wider Leverhulme Hyporheic Zone Network Team, Chithurst Buddhist Monastery, and Mr Ferguson for permitting access to their woodland, and two reviewers for comments that improved the manuscript.

#### ORCID

P.J. Blaen  <http://orcid.org/0000-0001-5748-3072>

D.M. Hannah  <http://orcid.org/0000-0003-1714-1240>

S. Krause  <http://orcid.org/0000-0003-2521-2248>

#### REFERENCES

- Battin, T. J., Kaplan, L. A., Findlay, S., Hopkinson, C. S., Marti, E., Packman, A. I., ... Sabater, F. (2008). Biophysical controls on organic carbon fluxes in fluvial networks. *Nature Geoscience*, 1, 95–100.
- Boano, F., Harvey, J. W., Marion, A., Packman, A. I., Revelli, R., Ridolfi, L., & Wörman, A. (2014). Hyporheic flow and transport processes: Mechanisms, models, and biogeochemical implications. *Reviews of Geophysics*, 52, 603–679.
- Buss, S., Cai, Z., Cardenas, B., Fleckenstein, J., Hannah, D., Heppell, K., ... Krause, S. (2009). *The hyporheic handbook: A handbook on the groundwater-surfacewater interface and hyporheic zone for environmental managers*. Bristol, UK: Environment Agency.
- Cardinale, B. J., Palmer, M. A., Swan, C. M., Brooks, S., & Poff, N. L. (2002). The influence of substrate heterogeneity on biofilm metabolism in a stream ecosystem. *Ecology*, 83, 412–422.

- Cole, J. J., Prairie, Y. T., Caraco, N. F., Mcdowell, W. H., Tranvik, L. J., Striegl, R. G., ... Middelburg, J. J. (2007). Plumbing the global carbon cycle: Integrating inland waters into the terrestrial carbon budget. *Ecosystems*, *10*, 172–185.
- Curran, J. H., & Wohl, E. E. (2003). Large woody debris and flow resistance in step-pool channels, Cascade Range, Washington. *Geomorphology*, *51*, 141–157.
- Dixon, S. J., & Sear, D. A. (2014). The influence of geomorphology on large wood dynamics in a low gradient headwater stream. *Water Resources Research*, *50*, 9194–9210.
- Dodds, W. K., Veach, A. M., Ruffing, C. M., Larson, D. M., Fischer, J. L., & Costigan, K. H. (2013). Abiotic controls and temporal variability of river metabolism: Multiyear analyses of Mississippi and Chattahoochee River data. *Freshwater Science*, *32*, 1073–1087.
- Drummond, J., Covino, T., Aubeneau, A., Leong, D., Patil, S., Schumer, R., & Packman, A. (2012). Effects of solute breakthrough curve tail truncation on residence time estimates: A synthesis of solute tracer injection studies. *Journal of Geophysical Research: Biogeosciences*, *117*.
- Fellows, C. S., Valett, M. H., & Dahm, C. N. (2001). Whole stream metabolism in two montane streams: Contribution of the hyporheic zone. *Limnology and Oceanography*, *46*, 523–531.
- Gomi, T., Sidle, R. C., & Richardson, J. S. (2002). Understanding processes and downstream linkages of headwater systems: Headwaters differ from downstream reaches by their close coupling to hillslope processes, more temporal and spatial variation, and their need for different means of protection from land use. *BioScience*, *52*, 905–916.
- González-Pinzón, R., Haggerty, R., & Argerich, A. (2014). Quantifying spatial differences in metabolism in headwater streams. *Freshwater Science*, *33*, 798–811.
- González-Pinzón, R., Peipoch, M., Haggerty, R., Martí, E., & Fleckenstein, J. H. (2016). Nighttime and daytime respiration in a headwater stream. *Ecohydrology*, *9*, 93–100.
- Grizzetti, B., Passy, P., Billen, G., Bouraoui, F., Garnier, J., & Lassaletta, L. (2015). The role of water nitrogen retention in integrated nutrient management: Assessment in a large basin using different modelling approaches. *Environmental Research Letters*, *10*, 065008.
- Haggerty, R., Argerich, A., & Martí, E. (2008). Development of a “smart” tracer for the assessment of microbiological activity and sediment-water interaction in natural waters: The resazurin-resorufin system. *Water Resources Research*, *44*.
- Hotchkiss, E. R., & Hall, R. O. Jr. (2014). High rates of daytime respiration in three streams: Use of  $\delta^{18}\text{O}_2$  and  $\text{O}_2$  to model diel ecosystem metabolism. *Limnology and Oceanography*, *59*, 798–810.
- Jin, L., Siegel, D. I., Lautz, L. K., & Otz, M. H. (2009). Transient storage and downstream solute transport in nested stream reaches affected by beaver dams. *Hydrological processes*, *23*, 2438–2449.
- Knapp, J. L., & Cirpka, O. A. (2017). Determination of hyporheic travel-time distributions and other parameters from concurrent conservative and reactive tracer tests by local-in-global optimization. *Water Resources Research*, *53*, 4984–5001. <https://doi.org/10.1002/2017WR020734>
- Krause, S., Klaar, M., Hannah, D., Mant, J., Bridgeman, J., Trimmer, M., & Manning-Jones, S. (2014). The potential of large woody debris to alter biogeochemical processes and ecosystem services in lowland rivers. *Wiley Interdisciplinary Reviews: Water*, *1*, 263–275.
- Lemke, D., Schnegg, P.-A., Schwientek, M., Osenbrück, K., & Cirpka, O. A. (2013). On-line fluorometry of multiple reactive and conservative tracers in streams. *Environmental earth sciences*, *69*, 349–358.
- Mendoza-Lera, C., Frossard, A., Knie, M., Federlein, L. L., Gessner, M. O., & Mutz, M. (2017). Importance of advective mass transfer and sediment surface area for streambed microbial communities. *Freshwater Biology*, *62*, 133–145.
- Mulholland, P., Fellows, C. S., Tank, J., Grimm, N., Webster, J., Hamilton, S., ... Dodds, W. (2001). Inter-biome comparison of factors controlling stream metabolism. *Freshwater Biology*, *46*, 1503–1517.
- Mulholland, P. J., Helton, A. M., Poole, G. C., Hall, R. O., Hamilton, S. K., Peterson, B. J., ... Dahm, C. N. (2008). Stream denitrification across biomes and its response to anthropogenic nitrate loading. *Nature*, *452*, 202–205.
- Piégay, H., & Gurnell, A. (1997). Large woody debris and river geomorphological pattern: Examples from SE France and S. England. *Geomorphology*, *19*, 99–116.
- R Core Team (2016). R: A language and environment for statistical computing. R Foundation for Statistical Computing, Vienna, Austria. 2015. [www.R-project.org](http://www.R-project.org).
- Rode, M., Halbedel NéE Angelstein, S., Anis, M. R., Borchardt, D., & Weitere, M. (2016). Continuous in-stream assimilatory nitrate uptake from high-frequency sensor measurements. *Environmental science & technology*, *50*, 5685–5694.
- Schmadel, N. M., Ward, A. S., Kurz, M. J., Fleckenstein, J. H., Zarnetske, J. P., Hannah, D. M., ... Schmidt, C. (2016). Stream solute tracer timescales changing with discharge and reach length confound process interpretation. *Water Resources Research*, *52*, 3227–3245.
- Schumer, R., Meerschaert, M. M., & Baeumer, B. (2009). *Fractional advection-dispersion equations for modeling transport at the Earth surface*. (p. 114). Journal of Geophysical Research: Earth Surface.
- Tank, J. L., Rosi-Marshall, E. J., Baker, M. A., & Hall, R. O. (2008). Are rivers just big streams? A pulse method to quantify nitrogen demand in a large river. *Ecology*, *89*, 2935–2945.
- Tank, J. L., Rosi-Marshall, E. J., Griffiths, N. A., Entekin, S. A., & Stephen, M. L. (2010). A review of allochthonous organic matter dynamics and metabolism in streams. *Journal of the North American Benthological Society*, *29*, 118–146.
- Ward, A. S., Gooseff, M. N., Voltz, T. J., Fitzgerald, M., Singha, K., & Zarnetske, J. P. (2013). How does rapidly changing discharge during storm events affect transient storage and channel water balance in a headwater mountain stream? *Water Resources Research*, *49*, 5473–5486.

## SUPPORTING INFORMATION

Additional Supporting Information may be found online in the supporting information tab for this article.

**How to cite this article:** Blaen PJ, Kurz MJ, Drummond JD, et al. Woody debris is related to reach-scale hotspots of lowland stream ecosystem respiration under baseflow conditions. *Ecohydrology*. 2018;11:e1952. <https://doi.org/10.1002/eco.1952>